INSTITUTE OF PHYSICS PUBLISHING JOURNAL OF PHYSICS G: NUCLEAR AND PARTICLE PHYSICS

J. Phys. G: Nucl. Part. Phys. **31** (2005) S1465–S1470 doi:10.1088/0954-3899/31/10/015

Structure of the neutron-rich Cr isotopes

S J Freeman[1], R V F Janssens[2], A N Deacon[1], F Xu[3], I J Calderin[5], M P Carpenter[2], P Chowdhury[6], S M Fischer[7], N J Hammond[2], M Honma[4], T Lauritsen[2], C J Lister[2], T LKhoo[2], G Mukherjee[2], D Seweryniak[2], J F Smith[1], S L Tabor[5], B J Varley[1] and S Zhu[2]

[1] Schuster Laboratory, University of Manchester, Manchester M13 9PL, UK
[2] Argonne National Laboratory, Argonne, IL-60439, USA
[3] Peking University, Beijing 100871, People's Republic of China
[4] University of Aizu, Fukushima 965-8580, Japan
[5] Florida State University, Tallahassee, FL-32306, USA
[6] University of Massachusetts, Lowell, MA-01854, USA
[7] DePaul University, Chicago, IL-60604, USA

E-mail: sjf@mags.ph.man.ac.uk

Received 15 March 2005
Published 12 September 2005
Online at stacks.iop.org/JPhysG/31/S1465

Abstract

The low-lying levels in ^{59,60}Cr have been populated with ^{13,14}C(^{48}Ca, 2p) reactions using a beam energy of 130 MeV. Prompt electromagnetic radiation was detected using the Gammasphere array, in coincidence with recoiling ions measured with the Fragment Mass Analyzer. The residues were selected and identified on the basis of charge-to-mass ratio, energy-loss and time-of-flight measurements. Preliminary results for ^{60}Cr, when compared to lighter even-even isotopes, indicate a softness in shape which increases with neutron number. The low-lying structure of ^{59}Cr is clearly inconsistent with the results of a spherical shell-model calculation and requires the inclusion of the $\nu g_{9/2}$ orbital. The sequence of states can be understood within the Nilsson model assuming a moderate oblate ground-state deformation. This is in contrast to lighter odd-Cr nuclei where there is evidence for prolate deformation after excitation of $g_{9/2}$ neutrons.

1. Introduction

Considerable effort is currently focused on developing a proper understanding of the structure of neutron-rich nuclei. Such studies reveal aspects of the nuclear force that are not readily apparent in stable and neutron-deficient systems. Applying the nuclear shell model to neutron-rich nuclei requires the development of novel effective interactions within new model spaces. Recent efforts to apply the full $\pi f_{7/2}\nu fp$ space to neutron-rich nuclei above doubly-magic ^{48}Ca typify such an approach [1]. In this particular case, the role of a strong π–ν monopole

interaction has been highlighted which causes significant shifts in the energy of the $\nu f_{5/2}$ state as the $\pi f_{7/2}$ orbital fills. This shift, when combined with a relatively low single-particle level density, conspires to produce an unexpected $N = 32$ subshell closure in Ca, Ti and Cr nuclei [2–4]. The success of calculations employing the fp model space depends sensitively on the size of the $N = 40$ subshell gap. A large gap effectively isolates the low-lying structure from the $\nu g_{9/2}$ orbital and would bode well for the efficacy of the fp space. On the other hand, a weak subshell closure facilitates single-particle excitations outside the model space, leading to difficulties with calculations that ignore the $\nu g_{9/2}$ level. Neutron excitations into the $g_{9/2}$ state should have clear structural consequences as this orbital has considerable potential for polarizing the nuclear shape via strong deformation-driving effects. The chromium isotopes lie in the middle of the $\pi f_{7/2}$ shell and would, therefore, be expected to display some of the strongest collective effects. Here we report on detailed studies of the structure of neutron-rich Cr isotopes where, contrary to previous claims of large stable ground-state deformation [5], the results indicate considerable softness in shape which appears to increase with neutron number. With such pliant cores, odd Cr isotopes are expected to show considerable polarization in shape when valence particles are excited into eccentric orbits, such as the $\nu g_{9/2}$ single-particle state, and evidence is found for such phenomena.

The production of neutron-rich isotopes still presents a major challenge. In this work the most neutron-rich stable targets and projectiles have been used to produce the most exotic compound nucleus possible. Most of the subsequent evaporation is via neutron emission taking the system back towards stability, but rare two-proton evaporation actually increases the proton deficiency of the residues. Very selective techniques are necessary to extract events associated with such weak channels.

2. Experimental details

The techniques employed in the production and identification of neutron-rich nuclei have been described in [6] where more details can be found. Beams of $^{48}Ca^{11+}$ ions were accelerated to energies of 130 MeV using the ATLAS accelerator at Argonne National Laboratory and used to bombard enriched $^{13,14}C$ targets, with approximate thicknesses of 100 μg cm^{-2}. In both cases, the isotopic enrichment was at a level of about 90%, the main contaminant being ^{12}C. Prompt γ rays were detected with the Gammasphere array. Ions recoiling from the target position were separated from primary beam particles and dispersed along a focal plane according to their charge-to-mass (A/q) ratio using the Fragment Mass Analyzer (FMA), which was tuned to transport ions with charge state 17+ and mass 60. A parallel-grid avalanche counter at the focal plane was used to measure the positions of the recoils, behind which a segmented ion chamber recorded their rate of energy loss. The data acquisition was triggered by an event corresponding to the arrival of an ion at the focal plane in coincidence with the detection of at least one γ ray in Gammasphere.

The isotopic selection techniques used will be discussed with the $^{14}C(^{48}Ca, 2p)^{60}Cr$ reaction as an example. The combination of the total ion energy, E, and the time of flight through the FMA, T, in the form ET^2 is proportional to the mass of the ion. This was used to help resolve charge-state ambiguities, as illustrated in figure 1(a), where the resolution in such a measurement is sufficient to separate the $A/q = 60/17$ ions from the $A/q = 56/16$ group. The atomic number of the recoiling ions is easily deduced from the energy-loss characteristics of the ions in the gas-filled ion chamber, as illustrated in figure 1(b). The Cr band in this plot has two distinct lobes which occur as the Cr yield is dominated by channels involving α evaporation; the acceptance of the FMA restricts the α-particle evaporation to tight cones, up and down the beam direction, leading to high- and low-energy Cr ion groups. Conditions

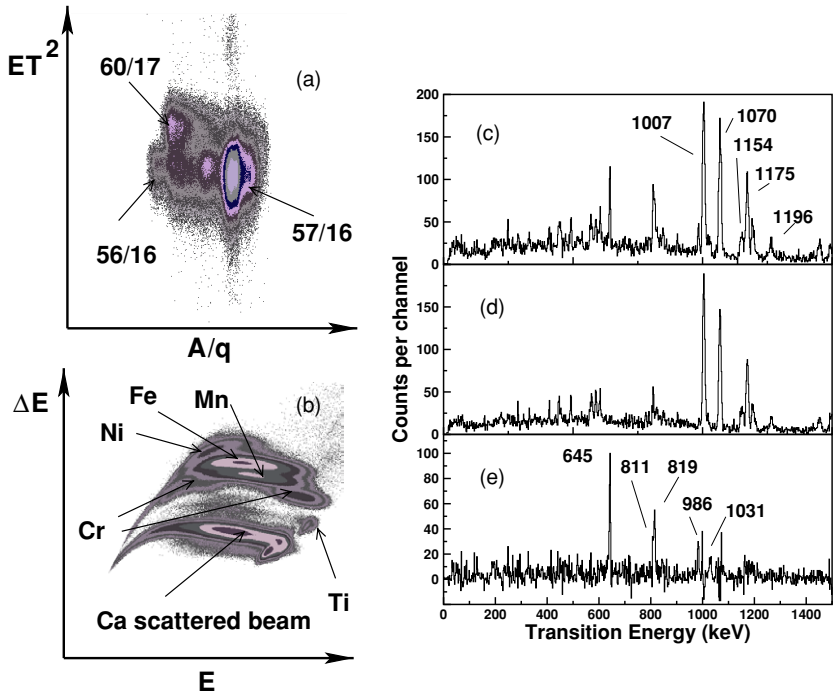

Figure 1. Two-dimensional plots for ion identification: (a) ET^2 versus charge-to-mass ratio, A/q, of ions. Various ion groups are labeled by A/q. (b) Energy loss versus total energy in the ionization chamber. All axes are in arbitrary units. Singles γ-ray spectra with various channel selection cuts applied are shown in the right-hand panel: (c) is gated by $A/q = 60/17$ and $Z = 24$, where transitions previously known in ^{56}Cr [10] are labelled by the transition energy quoted to the nearest keV, (d) is gated by $A/q = 56/16$ and $Z = 24$, and (e) is the normalized subtraction of (d) from (c) where transitions assigned to ^{60}Cr are indicated.

placed on the groups in figures 1(a) and (b) were used to select events corresponding to $A/q = 60/17$ and $Z = 24$ ions; coincident γ-ray transitions are illustrated in figures 1(c)–(e). Panel (c) shows the raw spectrum with these gates applied. It is clear that the tail of the considerably more intense $A/q = 56/16/Z = 24$ ion group leaks into this gate. The peaks arising from this channel have a noticeably larger width arising from a larger spread in recoil velocities associated with α-particle evaporation. Other lines are present which, without the ET^2 selection, would be obscured by the ^{56}Cr events. Figure 1(d) shows the spectrum gated on the tail of the $A/q = 56/16/Z = 24$ group, away from the $A = 60$ peak, clearly identifying the leak-through peaks. Figure 1(e) presents a normalized subtraction of these two spectra; peaks in this spectrum are, therefore, assigned as transitions in ^{60}Cr. Further evidence for the mutual association of these transitions can be obtained through analysis of γ–γ coincidences. Although the data are sparse, the level of statistics is sufficient to establish level schemes. An example of such an analysis is presented in [6].

3. Results

The level schemes, deduced from both recoil-γ and recoil-γ–γ data (the latter is not discussed in detail here), are shown in figures 2(a) and (b) [6]. These results represent significant extensions of previous work, which had established only a 646 keV transition in ^{60}Cr [5] and

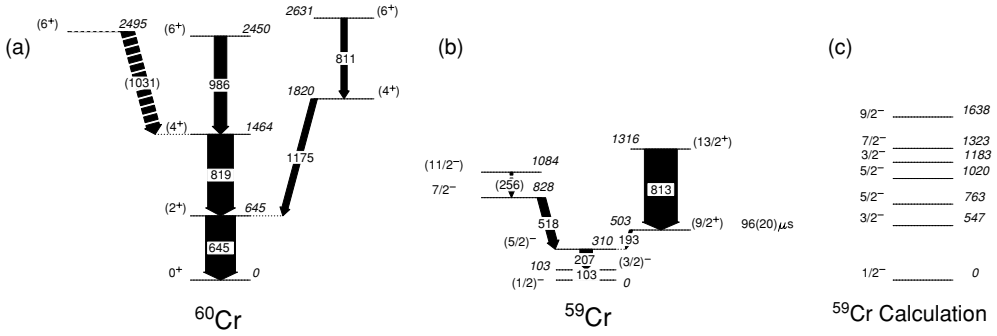

Figure 2. Energy levels in neutron-rich chromium isotopes. (a) The ^{60}Cr level scheme. (b) The ^{59}Cr level scheme [6]. (c) Energy levels of ^{59}Cr from a shell-model calculation within the full fp-shell basis using the GXPF1A interaction [8]. Spins of states in ^{60}Cr were assigned on the basis of yrast feeding, whereas those in ^{59}Cr are based on more detailed model-dependent arguments [6].

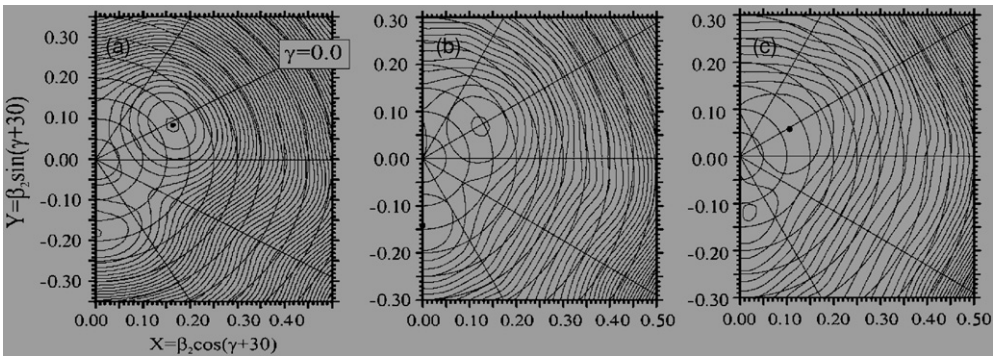

Figure 3. The potential energy surface arising from TRS calculations for yrast, positive-parity configurations in (a) ^{56}Cr, (b) ^{58}Cr and (c) ^{60}Cr at a rotational frequency of 0.0 MeV/$\hbar$. Contours are shown at 200 keV intervals and a dot is used to illustrate the absolute minimum.

two prompt transitions at 103 and 207 keV in ^{59}Cr [7]. No evidence was presented for the ordering of these transitions in ^{59}Cr.

The structure of ^{60}Cr appears to cast doubt on interpretations involving well-developed oblate deformation. Whilst arguments on the basis of the first 2^+ energy and simple systematics presented in [5] might suggest a large oblate shape, the low-lying structure of ^{60}Cr does not have characteristic features that would be associated with a well-developed stable oblate configuration. The $E(4^+)/E(2^+)$ ratio, for example, is only 2.27. If oblate deformation is present, the observed structure suggests significant mixing with other shapes. Total Routhian surface (TRS) calculations have been performed and the results are consistent with these characteristics. The TRS results for low rotational frequency are shown in figure 3, where it is clear that the potential energy surfaces for the neutron-rich Cr isotopes are rather soft and get progressively softer with neutron number, particularly in the γ degree of freedom.

The low-lying structure of ^{59}Cr should reflect single-neutron excitations within the fp-shell orbitals, along with $1g_{9/2}$, depending on the strength of the $N = 40$ closure. β decay feeds the $5/2^-$ state at 310 keV and possibly the $3/2^-$ state at 103 keV [7], suggesting an $f_{5/2}$ parentage for at least the $5/2^-$ state via allowed $\pi f_{7/2} \rightarrow \nu f_{5/2}$ decays. Calculations, performed within the full fp-shell basis using the GXFP1A interaction [8], are shown in figure 2(c). Although

the spin and parity of the ground state are reproduced, comparison with experiment reveals a failure to provide a description of the low-lying states. Furthermore the low-lying $9/2^+$ state is very obviously outside of the fp-model space. Observation of this state at such a low excitation energy, suggests the presence of deformation. For small oblate deformations within a deformed Woods–Saxon calculation [6], the $9/2^+$ state from this orbital falls dramatically in energy towards the Fermi surface to energies consistent with the experimental observation. The ground and other low-lying excited states also appear consistent with a moderate oblate ground-state deformation [6].

It is interesting to compare the behaviour of the yrast $9/2^+$ state in ^{59}Cr with that in the lighter isotopes, in particular, ^{57}Cr which is produced by αn evaporation following the reaction on ^{14}C. The details can be found in a forthcoming publication [9], but to summarize, the $9/2^+$ state lies at 1.506 MeV and γ–γ coincidence methods have established a regular sequence of transitions built upon it. This band has features of a decoupled rotational band based upon the $1/2^+$ [440] Nilsson orbital. A prolate deformation is deduced on the basis of the rotational character of the sequence of states, the decoupled nature of the bands and the reproduction of their rotational behaviour with TRS calculations. Such calculations also reproduce the properties of a similar, but less well-developed structure in ^{55}Cr [10]. In ^{59}Cr, a prolate state is incompatible with the isomeric nature of the $9/2^+$ state as in-band transitions would be available for its decay. It appears that the excitation of a $g_{9/2}$ neutron drives an already mildly oblate core further towards oblate deformation. Further evidence for an oblate nature would be the observation of a coupled band structure built on the isomer; however, a only a single tentative transition has so far been observed [6]. These abrupt changes in structure appear as a result of the low single-particle level density which leads to energy gaps in the level structure at both oblate and prolate deformation. Similar phenomena are seen in $N = Z$ nuclei with $A \sim 80$, where protons *and* neutrons fill the same orbits as neutrons do here. In this heavier region, strong π–ν interactions reinforce the shell gaps leading to a well-defined deformation, even in the ground states. The lack of such cooperative effects near $A \sim 60$ in neutron-rich nuclei masks the effect of these gaps, producing soft cores where ground-state deformation, if present, is small. Polarization by an excited nucleon in a deformation-driving orbit is then required to make the full extent of the collective effects apparent.

The cross sections inferred from the observed yields for the ^{13,14}C(^{48}Ca, 2p) reactions are approximately 10 and 5 μb respectively, assuming an FMA transmission of 5% in each case. This is the first time that such multiple charged-particle evaporation channels have been isolated in this region and prove to be a viable route with which to perform spectroscopy. The information gathered here is clearly more extensive than previous studies of fragmentation products. Deep-inelastic reactions can penetrate into this region, but thick-target experiments have suffered from the lack of isotopic identification, unless at least one γ-ray transition is already known. Some of the transitions observed here can be seen in reactions of ^{48}Ca on ^{238}U at beam energies of 25% above the fusion barrier, given the isotopic identification of transitions gained in the current work [11]. The extension of these identification methods to the 3p channel requires increased beam energy. The use of the FMA in such cases would require degradation of the recoil energy prior to entering the separator. Whilst not being impossible, this would require development given the particular issues with scattered beam in these inverse reactions.

Acknowledgments

This work was supported by the UK EPSRC, the US National Science Foundation under Grant Nos PHY-0244453 and PHY-0139950, and the US Department of Energy, Office of Nuclear

Physics under contract W31-109-ENG-38 and DE-FG02-94ER40848. The authors would like to thank University of Birmingham for the use of their ^{14}C target.

References

[1] Honma M *et al* 2002 *Phys. Rev.* C **65** 061301
[2] Janssens R V F *et al* 2002 *Phys. Lett.* B **546** 55
[3] Liddick S N *et al* 2004 *Phys. Rev.* C **70** 064303
[4] Fornal B *et al* 2004 *Phys. Rev.* C **70** 064304
[5] Sorlin O *et al* 2003 *Eur. J. Phys.* **16** 55
[6] Freeman S J *et al* 2004 *Phys. Rev.* C **69** 064301
Freeman S J *et al* 2004 *Phys. Rev.* C **70** 029901E
[7] Sorlin O *et al* 2000 *Nucl. Phys.* A **669** 351
[8] Honma M 2004 *Proc. Int. Conf. on Exotic Nuclei and Atomic Masses* (*Eur. Phys. J.*, in press)
[9] Deacon A N *et al* 2005 at press
[10] Appelbe D E *et al* 2003 *Phys. Rev.* C **67** 034309
[11] Zhu S and Janssens R V F 2005 Private communication